THE JOURNAL OF PHYSICAL CHEMISTRY A

ARTICLE

pubs.acs.org/JPCA

Noncovalent Interactions between Modified Cytosine and Guanine DNA Base Pair Mimics Investigated by Terahertz Spectroscopy and Solid-State Density Functional Theory

Matthew D. King and Timothy M. Korter*

Department of Chemistry, Syracuse University, 1-014 Center for Science & Technology, 111 College Place, Syracuse, New York 13244-4100, United States

Supporting Information

ABSTRACT: Modified cytosine and guanine nucleobases cocrystallize in a hydrogen bonding configuration similar to that observed in native DNA. The noncovalent interactions binding these base pairs in the crystalline solid were investigated using terahertz (THz) spectroscopy and solid-state density functional theory (DFT). While stronger hydrogen bonding interactions are responsible for the general molecular orientations in the crystalline state, it is the weaker dipole−dipole and dispersion forces that determine the overall packing arrangement. The inclusion of dispersion interactions in the DFT calculations was found to be necessary to accurately simulate the unit cell structure and THz vibrational spectrum. Using properly modeled intermolecular potentials, the lattice vibrational motions of the cytosine and guanine derivatives were calculated. The vibrational characters of the modes exhibited by the DNA base pair mimic in the THz region were primarily rotational motions and are indicative of the energies and the nature of vibrations that would likely be observed between similar base pairs in DNA molecules.

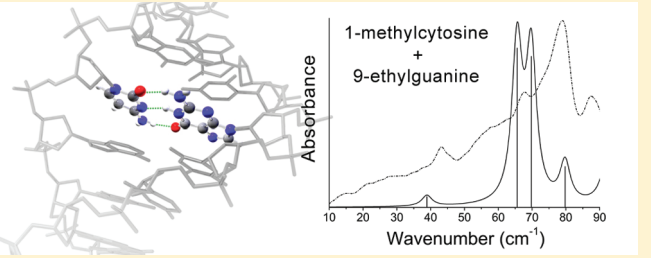

INTRODUCTION

Noncovalent forces are critical in biological systems and are responsible for the highly specific structure and functionality of large molecular complexes, such as DNA and proteins. The vitally important and intricate interactions within and between biomolecules are of great interest and inspire the continual development of spectroscopic techniques set to uncover the structural dynamics of such systems. The recent progression of ultrafast laser technology has rapidly advanced the application of many valuable analytical techniques, including terahertz (THz) spectroscopy.[1−3] With the ability to probe low-frequency vibrations, THz spectroscopy can be used to obtain information about the intermolecular interactions present in condensed-phase systems.[4−7] Molecules of biological importance, such as amino acids,[8−11] nucleic acids,[12−14] and pharmaceuticals,[15−18] have been the subjects of many THz spectroscopic investigations. While most biosystems under investigation by THz spectroscopy are still relatively small, with improvements in the theoretical interpretations of THz spectra will come the enhancement of our understanding of the elaborate dynamics within increasingly complex molecular structures.[19,20]

In this study, the cocrystal of modified DNA nucleobases, 1-methylcytosine (C) and 9-ethylguanine (G), were studied via THz spectroscopy. These bases form a hydrogen bonding pattern between the modified C and G molecules in the same manner as found in native DNA molecules. The strongly hydrogen bonded base pairs are held in the crystalline solid by weaker noncovalent interactions. The modifications to the C and G molecules include the additions of methyl and ethyl groups, respectively, at the location of the glycosidic attachment to these molecules as they are found in DNA molecules. The goal was to investigate the nature of the vibrational motions exhibited by DNA nucleobases in this model hydrogen bonding configuration, providing insight into vibrational motions that might occur between these molecules when incorporated into larger DNA molecules. This investigation follows a recently published THz study of the cocrystal formed by modified adenine (A) and thymine (T) base pairs, which found several concerted rigid-body rotational motions of the base pairs below 100 cm^{-1}.[21] It was, therefore, deemed appropriate to analyze the 1-methylcytosine:9-ethylguanine 1:1 cocrystal (CG) in the same manner.

The THz spectrum of CG was obtained from 10 to 90 cm^{-1} at room temperature and at 78 K. The vibrational motions of crystalline CG leading to absorptions in the THz region were calculated using solid-state density functional theory (DFT) with periodic boundary conditions, which has been shown to consistently produce accurate simulations of crystal structures and THz spectra.[22−24] Using DFT augmented with a $1/R^6$ dispersion correction term, the influence of weak London-type dispersion interactions on the structure and vibrational modes were carefully

Received: September 14, 2011
Revised: October 27, 2011
Published: November 22, 2011

evaluated.[25,26] Since these forces are essential for the arrangements of molecules in the solid state, as well as the organization of large biological complexes, it is important that these forces be accounted for in the solid-state DFT calculations. It was discovered for the previously reported AT cocrystal that dispersion forces were essential for the arrangement and stabilization of the individual molecules in the crystalline structure.[21] Without the inclusion of these forces, meaningful simulations of the THz spectrum would not have been possible for this system. Given these results, one would tend to believe that the same would hold true for the calculations of the similar CG cocrystal.

The DFT calculations of the 1:1 cocrystal of CG were performed both with and without corrections for dispersion forces. Without these important interactions, the structural optimization led to the considerable asymmetric expansion of the unit cell volume. The resulting ill-represented arrangement of the CG molecules produced a very poor simulation of the experimental THz spectrum. However, when including the dispersion correction term in the DFT calculations, the simulated crystal structure and THz spectrum were both in good agreement with experimental observations. These results are consistent with previous findings in which dispersion forces were necessary to properly model crystals of DNA components and their corresponding vibrational spectra using solid-state DFT.

MATERIALS AND METHODS

Experimental Section. 1-Methylcytosine (no. dn044) was purchased from SYNCHEM OHG, 9-ethylguanine (no. sc-207221) was purchased from Santa Cruz Biotechnology, Inc., and dimethyl sulfoxide (DMSO, no. D128-500) was purchased from Fisher Scientific. All chemicals were used without further purification. 1:1 CG cocrystals were grown by evaporation of an equimolar DMSO solution at 80 °C.[27]

Experimental THz spectra were obtained using a time-domain pulsed THz spectrometer based on an amplified Ti:Sapphire femtosecond near-infrared laser system. ZnTe crystals were used for generation of THz radiation by optical rectification[28] and detection by free-space electrooptic sampling.[29] A detailed description of the THz spectrometer has been reported elsewhere.[30]

Samples for THz measurements were mixed with polytetrafluoroethylene (PTFE) powder at a concentration of approximately 5% by mass and pulverized using a stainless-steel ball mill (Dentsply Rinn 3110-3A) to minimize particle size, thereby reducing nonresonant scattering of THz radiation. Approximately 0.55 g of the sample mixtures was pressed into pellets under a measured pressure of 2000 psi (~10 000 psi at sample) using a hydraulic press (ICL EZ-Press 12) equipped with a 13-mm stainless steel die, giving final pellet dimensions of 13 mm × 2.2 mm. Pure PTFE pellets for use as "blank" references were prepared in the same manner. The samples and blanks for measurement were held in a cryostat (Janis Research Systems) equipped with 3-mm thick polymethylpentene windows. Data were acquired at 293 and 78 K with samples under vacuum. Samples and blanks were scanned 32 times and data averaged for each individual data set. A 32 ps scan window consisting of 3200 data points was used to capture the THz waveform, which was then symmetrically zero-padded to a total of 6000 data points for the data transforms. The effective instrument resolution arising from the 32 ps scan length was approximately 1.0 cm^{-1}. Fourier transforms were performed using a Hanning window. The ratio of the power spectra obtained from the Fourier-transformed data sets of the sample and blank yielded the THz absorption spectrum. Each THz spectrum presented in this work is the average of four individual THz spectra, each representing a complete set of sample and blank measurements.

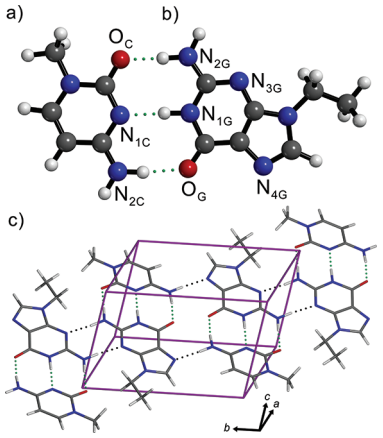

Figure 1. Hydrogen bonded dimer of (a) 1-methylcytosine and (b) 9-ethylguanine, and atom labels used in bonding descriptions. (c) Unit cell and hydrogen bonding arrangement of 1-methylcystosine and 9-ethylguanine 1:1 cocrystal.

Theoretical. All DFT calculations were performed using the CRYSTAL09 software package.[31,32] Calculations utilized the PBE density functional[33] with the atom-centered 6-311G(d,p) basis set.[34] Calculations incorporating an empirical dispersion correction term of the form C_6/R^6 are denoted as PBE-D throughout.[25,26] Parameters for the dispersion correction term are provided in the Supporting Information.[26,35] A value of 0.55 was used for the functional-dependent global dispersion scalar (s_6) of the dispersion term based on previous studies, including that of the related adenine:thymine cocrystal.[21,36] Initial atomic positions and lattice parameters were taken from the previously reported cocrystal structure available from the Cambridge Structural Database (EGMCYT10).[27] The reported lattice dimensions for the CG cocrystal system were a = 8.838 Å, b = 11.106 Å, c = 7.391 Å, α = 107.82°, β = 87.05°, and γ = 91.45°. Structural optimizations were performed both with and without corrections for dispersion forces. For these optimizations, all lattice dimensions were allowed to fully relax while preserving imposed $P\bar{1}$ space group symmetry.

Total energy convergence criteria of $\Delta E < 10^{-8}$ hartree was used for geometry optimizations and $\Delta E < 10^{-11}$ hartree for normal mode calculations. Shrinking factors for reciprocal lattice vectors were set to values of 4 to specify the sampling rate as a function of **k** points in defining the Pack−Monkhorst and Gilat nets.[37,38] The radial and angular distribution of points was defined by a pruned (75, 974) integration grid. Truncation tolerances used for Coulomb and HF exchange integral series were set to 10^{-6}, 10^{-6}, 10^{-6}, 10^{-6}, and 10^{-12} hartree.[39] Frequencies of normal modes were calculated within the harmonic approximation by numerical differentiation of the analytical gradient of the potential energy with respect to atomic position.[40] The IR intensities for normal modes were calculated from the dipole moment derivatives ($d\mu/dQ$) determined using the Berry phase approach to calculate the Born charge tensors.[41]

RESULTS AND DISCUSSION

Terahertz Spectroscopy. The THz spectrum from 10 to 90 cm^{-1} of the CG cocrystal was obtained at room temperature

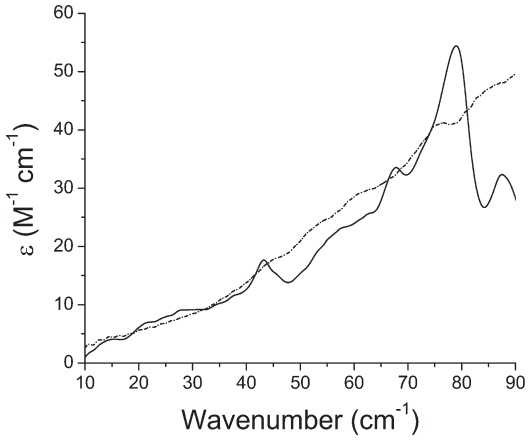

Figure 2. Terahertz spectra from 10 to 90 cm^{-1} of 1-methylcystosine and 9-ethylguanine 1:1 cocrystal at 293 K (dashed line) and 78 K (solid line).

and 78 K (Figure 2). At room temperature, a rising baseline in the spectrum masked the absorptions due to CG, although some features are actually present and only became discernible at reduced temperature. When the sample was cooled to liquid-nitrogen temperatures, the reduction in peak width and baseline revealed four spectral features at 43.3, 67.6, 78.9, and 88.2 cm^{-1}. Small baseline features not resulting from absorption due to vibrational motions of CG could be attributed to background noise because the absorption intensities do not scale linearly with sample concentration. The background noise also varied between individually prepared samples. The significant rising baselines in the spectra are not unusual in THz spectroscopy. Possible sources contributing to the background noise and baseline may include poor quality CG cocrystals or a large crystallite size distribution in the sample due to insufficient pulverization leading to nonresonant radiation scattering. Regardless, the four vibrational mode locations can be easily distinguished in the THz spectrum obtained at 78 K.

Structural Analysis. The molecules in the 1:1 CG cocrystal are arranged in a dense, close-packing arrangement. The C and G molecules form planar dimers joined by three hydrogen bonds analogous to the configuration observed naturally in DNA between cytosine and guanine base pairs (Figure 1). The ordered pairs are arranged in continuous chains, connected through weak N−H···N contacts. These chains are closely stacked in the crystalline solid and are held together primarily through dispersion interactions. The $P\bar{1}$ unit cell consists of two C···G pairs ($Z = 4$) related by an inversion center. The irreducible asymmetric unit consists of one complete C···G pair.

It has been argued in some THz spectroscopic studies of biological molecules utilizing solid-state DFT that full unit cell optimizations do not require the inclusion of dispersion corrections.[11,42] In rare cases, it may be found that for strongly hydrogen bonded systems, optimal directionality of hydrogen bonding forces, which are well modeled by DFT, may reduce the need for explicit dispersion forces.[11] However, it has been compellingly put forth that for most molecular crystal systems, dispersion forces are critical for the reproduction of unit cell structures and THz spectra.[21,36,43] Geometry optimizations were performed by both PBE and PBE-D methods for the CG cocrystal to further demonstrate the necessity of these weak stabilizing forces to be incorporated into the computational methods for molecular solids.

Table 1. Lattice Dimensions for 1-Methylcystosine and 9-Ethylguanine 1:1 Cocrystal from Full Unit Cell Optimizations Using PBE and PBE-D[a]

				Δ (%)	
	exp[b]	PBE-D	PBE	PBE-D	PBE
a (Å)	8.838	8.8746	9.9537	0.414	12.624
b (Å)	11.106	10.9581	10.5818	−1.332	−4.720
c (Å)	7.391	7.1539	7.6439	−3.208	3.422
α (deg)	107.82	104.081	93.423	−3.47	−13.35
β (deg)	87.05	87.746	98.525	0.80	13.18
γ (deg)	91.45	91.706	89.165	0.28	−2.50
V (Å^3)	689.7	674.14	794.80	−2.3	15.2
d (g cm^{-3})	1.464	1.498	1.271	2.322	−13.183

[a] Difference between calculated and experimental lattice dimensions given as a percentage. [b] Experimental taken from ref 26.

The full-geometry optimizations using PBE without dispersion forces yielded a greatly distorted unit cell as compared to the experimental structure (Table 1). Variations in unit cell dimensions as large as 12.6% were observed along the lattice vectors, and 13% for lattice angles. The resulting unit cell had a volume 15.2% greater (which corresponds to a 13.2% lower density) than that of the experimentally determined cell. The very poor reproduction of the unit cell structure was clearly due to the neglect of dispersion interactions, as these forces are determining factors forming the close-packing arrangement exhibited in the CG cocrystal. Even though dispersion forces are not present in the calculations, the unit cell optimization did reach an energetic minimum, although not with an accurate portrayal of the physical nature of the molecular system. The "optimized" unit cell dimensions are the product of misrepresented binding forces in the solid that are likely a combination of dipole−dipole interactions and false attractive contributions provided by the PBE functional formulation and basis set superposition error from the finite basis set.

The CG unit cell optimized using PBE-D showed that including dispersion forces in the calculations will supply a better representation of true crystal packing forces and, therefore, produce a more accurate crystal structure (Table 1). The average percent change in the optimized lattice vectors was 1.65% compared to the experimental values. The largest deviation of only 0.24 Å was observed along the c-axis. The lattice angles were also much better reproduced, averaging only a 1.5% error compared to the 9.7% for the PBE optimization. The resulting unit cell volume was decreased by a reasonable 2.3%, or 15.6 Å^3. The overall contraction of the unit cell was likely due to the magnitude of the dispersion correction term. Because the starting dimensions are that of the room-temperature structure, full geometry optimizations including dispersion corrections will most often result in the contraction of the unit cell structure. As there are no temperature contributions in the DFT model, scaling the magnitude of the dispersion correction may be used to compensate for this deficiency, albeit not an ideal solution to the problem.[21,36] The dispersion scalar value used in the PBE-D calculations of the CG system was based on previously reported calculations on the structurally similar adenine:thymine cocrystal. In this previous study, dispersion scalar values were optimized to reproduce 100 K unit cell structures. Thus, the contraction of the CG unit cell structure from the room-temperature dimensions

Table 2. Hydrogen Bonding Heavy Atom Distances (Å) for Calculated Structures Compared to the Experimental Structure

	exp[a]	PBE	PBE-D
$O_C\cdots N_{2G}$	2.806	2.825	2.790
$N_{1C}\cdots N_{1G}$	2.924	2.902	2.886
$N_{2C}\cdots O_G$	2.943	2.895	2.895
$N_{2C}\cdots N_{3G}$	2.993	3.018	2.957
$N_{2C}\cdots N_{4G}$	3.010	3.094	3.033

[a] Experimental structure.

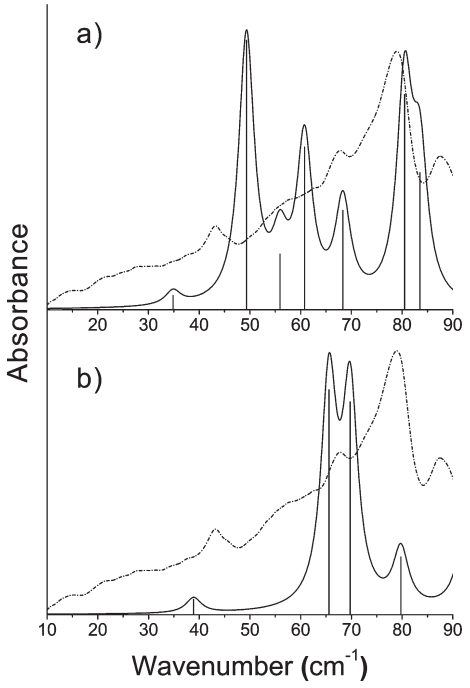

Figure 3. Experimental 78 K terahertz spectrum (dashed line) overlaid with simulated terahertz spectra (solid lines) of 1-methylcystosine and 9-ethylguanine 1:1 cocrystal calculated using (a) PBE without corrections for dispersion forces, and (b) PBE-D. The simulated spectral intensities are scaled to match experimental intensities for ease of comparison. Lorentzian line shapes with empirically determined full-width half-maximum values of 3.7 cm^{-1} were convolved into calculated modes.

would suggest a likewise reproduction of the approximate 100 K crystal structure.

The experimentally observed hydrogen bonding distances were maintained in both the PBE and PBE-D optimizations (Table 2). This shows the ability of DFT to accurately represent strong electrostatic interactions. Therefore, the changes in unit cell dimensions in the full-geometry optimizations are due to the misrepresentation of weaker dispersive interactions responsible for the molecular packing in the CG crystal structure. The results obtained from the structural optimizations illustrated the importance of dispersion forces in the arrangement of molecules in the solid state. This reproduction of unit cell structure is also critical for the accurate simulation of THz spectra.[21,36] This sensitivity is demonstrated here by performing normal mode calculations using the crystal structures optimized by both the PBE and PBE-D methods.

Table 3. Experimental and Calculated IR-Active Vibrational Modes from 10 to 90 cm^{-1} for the 1-Methylcystosine and 9-Ethylguanine 1:1 Cocrystal

		PBE-D		PBE	
mode[a]	exp[b]	freq[c]	int[d]	freq	int
ν_1	43.3	38.90	0.93	34.85	1.22
ν_2	67.6	65.58	13.64	49.33	22.97
ν_3	78.9	69.76	12.92	55.92	4.74
ν_4	88.2	79.76	3.51	60.76	13.87
				68.33	8.47
				80.50	18.35
				83.43	11.68

[a] Mode labels correspond to PBE-D modes only. [b] Experimental frequencies (cm^{-1}); [c] Frequency (cm^{-1}); [d] Intensity (km mol^{-1}).

THz Spectral Simulations. Using the poorly reproduced crystal structure from the PBE optimization, the resulting THz spectral simulation could not be correlated with the experimental spectrum (Figure 3a). A total of seven IR-active modes were calculated between 10 and 90 cm^{-1}, all with appreciable absorption intensities (Table 3). Some of the mode frequencies are similar to the experimental absorptions; however, the multiple high-intensity modes calculated below 65 cm^{-1} are inconsistent with experimental observations. The calculated intensities displayed in Figure 3a were scaled down by a factor of 2.35, which shows the considerably large estimation of absorption intensities for these calculated modes. It is unlikely that the THz vibrational modes calculated using the PBE structure are representative of the true normal modes of vibration exhibited by the CG system.

A much more reasonable spectral simulation was achieved from the vibrational modes calculated using the PBE-D optimized crystal structure (Figure 3b). Four IR-active modes were calculated with locations and intensities that were in agreement with the experimental spectrum (Table 3). Although the vibrational frequencies were all slightly underestimated, each mode could be assigned to an experimental absorption. Mode ν_1 calculated at 38.90 cm^{-1} was assigned to the experimental feature at 43.3 cm^{-1}. The two nearly equally intense calculated modes ν_2 and ν_3 were assigned to the absorptions centered at 67.6 and 78.9 cm^{-1}, respectively. The relative intensity of vibrational mode ν_2 was overestimated by the calculations. The experimental absorption at 88.2 cm^{-1} was assigned to mode ν_4 calculated at 79.76 cm^{-1}. With these assignments, the root-mean-squared deviation of calculated frequencies was 6.7 cm^{-1}. Accounting for the systematic underestimation, an optimum frequency scalar of 1.106 reduces the deviation to 2.6 cm^{-1}. Overall, the calculated intensities were also in very good agreement with experiment. The mode intensities shown in Figure 3b were reduced by a factor of only 1.3. Given the spectral overlap of the two highest intensity modes, the agreement between the simulated and experimental spectra are in even better agreement than the intensity scalar indicates.

The vibrational motions exhibited in the four IR-active modes calculated by PBE-D consist mainly of molecular rotations (Table 4). These rigid-body rotations are primarily modulated by the strong hydrogen bonding between the 1-methylcytosine and 9-ethylguanine molecules. The characters of the vibrational motions are analogous to those observed in paired adenine and thymine derivatives.[21] The motions of CG and AT base pairs in

Table 4. Mode Descriptions for the IR-Active Vibrational Modes Based on the PBE-D Calculation

mode	freq[a]	symm[b]	mode character[c]
ν_1	38.90	A_u	in-phase rotations about *a*-axis
ν_2	65.58	A_u	out-of-phase rotations about *b*-axis
ν_3	69.76	A_u	in-phase rotations about *c*-axis
ν_4	79.76	A_u	in-phase rotations about *b*-axis

[a] Frequency (cm^{-1}). [b] Symmetry. [c] Phase corresponding to hydrogen-bonded C···G pair.

the solid state are not unlike the vibrational motions that would be seen between nucleotide bases in DNA molecules. The results of these two studies suggest that DNA molecules should exhibit collective base pair rotational motions in the spectral range below 90 cm^{-1} that could be probed by THz spectroscopy. However, the exact vibrational frequencies would vary from those observed in the cocrystalline solids due to differences in the local molecular environment modifying the intermolecular contacts.

The inability to reproduce the THz spectrum without the incorporation of dispersion forces is telling of the importance of such forces in molecular solids. Even though the strong hydrogen bonding contacts were similarly reproduced in both the PBE and PBE-D structural calculations, the positioning of non-hydrogen bonded components were changed considerably in the absence of dispersion forces, made evident by the large change in unit cell dimensions in the PBE optimization. The improper molecular arrangements resulting from the PBE optimization led to the calculation of erroneous vibrational modes. Weak dispersion interactions have a large influence on lattice vibrational motions and cannot be ignored in the simulation of crystal structures and THz spectra.

The dispersion interactions that are vitally important for the structure and function of biomolecules have been shown in this study to be equally important in the formation of crystalline solids composed of their constituent monomers. The same hydrogen bonding and base-stacking configurations observed between DNA base pairs are also seen in the cocrystals of the modified base pairs. Better understanding of simplified biomolecular systems will gradually lead to the proper interpretation of THz spectra of more complex systems. While still far from deciphering vibrational motions in large DNA molecules using these techniques, this study serves as a benchmark for studies of DNA base pairing interactions using THz spectroscopy.

CONCLUSIONS

The 1:1 cocrystal of the modified DNA base pair 1-methylcytosine and 9-ethylguanine were studied using THz spectroscopy and solid-state DFT. The hydrogen bonding between these molecules in the cocrystal is similar to that in native DNA molecules. In the spectral range of 10 to 90 cm^{-1}, four absorptions were observed. The DFT simulations showed that these absorptions arise from molecular rotations of the constituent molecules. It was also revealed in the DFT calculations that dispersion forces are necessary to accurately reproduce both the crystalline structure and the THz spectra of this system. The neglect of dispersion forces resulted in a very poorly reproduced crystal structure and an erroneous spectral simulation that could not be correlated to experimental spectrum. The inclusion of these important dispersion forces, however, provided an accurate description of the intermolecular forces, enabling the proper interpretation of the THz spectrum of the CG cocrystal.

ASSOCIATED CONTENT

Supporting Information. Additional information as noted in the text. This material is available free of charge via the Internet at http://pubs.acs.org.

AUTHOR INFORMATION

Corresponding Author
*E-mail: tmkorter@syr.edu.

ACKNOWLEDGMENT

This research was funded by a grant from the National Science Foundation CAREER Program (CHE-0847405). The authors also thank Syracuse University for continued support.

REFERENCES

(1) Beard, M. C.; Turner, G. M.; Schmuttenmaer, C. A. *J. Phys. Chem. B* **2002**, *106*, 7146.
(2) Plusquellic, D. F.; Siegrist, K.; Heilweil, E. J.; Esenturk, O. *ChemPhysChem* **2007**, *8*, 2412.
(3) Siegrist, K.; Bucher, C. R.; Mandelbaum, I.; Hight Walker, A. R.; Balu, R.; Gregurick, S. K.; Plusquellic, D. F. *J. Am. Chem. Soc.* **2006**, *128*, 5764.
(4) Fumino, K.; Peppel, T.; Geppert-Rybczynska, M.; Zaitsau, D. H.; Lehmann, J. K.; Verevkin, S. P.; Koeckerling, M.; Ludwig, R. *Phys. Chem. Chem. Phys.* **2011**, *13*, 14064.
(5) Yamaguchi, S.; Tominaga, K.; Saito, S. *Phys. Chem. Chem. Phys.* **2011**, *13*, 14742.
(6) Walther, M.; Fischer, B. M.; Uhd Jepsen, P. *Chem. Phys.* **2003**, *288*, 261.
(7) Witko, E. M.; Korter, T. M. *J. Phys. Chem. A* **2011**, *115*, 10052.
(8) King, M. D.; Hakey, P. M.; Korter, T. M. *J. Phys. Chem. A* **2010**, *114*, 2945.
(9) Rungsawang, R.; Ueno, Y.; Tomita, I.; Ajito, K. *J. Phys. Chem. B* **2006**, *110*, 21259.
(10) Ueno, Y.; Rungsawang, R.; Tomita, I.; Ajito, K. *Anal. Chem.* **2006**, *78*, 5424.
(11) Williams, M. R. C.; True, A. B.; Izmaylov, A. F.; French, T. A.; Schroeck, K.; Schmuttenmaer, C. A. *Phys. Chem. Chem. Phys.* **2011**, *13*, 11719.
(12) Fischer, B. M.; Walther, M.; Jepsen, P. U. *Phys. Med. Biol.* **2002**, *47*, 3807.
(13) Shen, Y. C.; Upadhya, P. C.; Linfield, E. H.; Davies, A. G. *Appl. Phys. Lett.* **2003**, *82*, 2350.
(14) Wilk, R.; Stewing, F.; Rutz, F.; Kleine-Ostmann, T.; Koch, M. *Int. J. Nanotechnol.* **2005**, *2*, 303.
(15) Strachan, C. J.; Taday, P. F.; Newnham, D. A.; Gordon, K. C.; Zeitler, J. A.; Pepper, M.; Rades, T. *J. Pharm. Sci.* **2005**, *94*, 837.
(16) Taday, P. F.; Bradley, I. V.; Arnone, D. D.; Pepper, M. *J. Pharm. Sci.* **2003**, *92*, 831.
(17) Wallace, V. P.; Taday, P. F.; Fitzgerald, A. J.; Woodward, R. M.; Cluff, J.; Pye, R. J.; Arnone, D. D. *Faraday Discuss.* **2004**, *126*, 255.
(18) Zeitler, J. A.; Newnham, D. A.; Taday, P. F.; Threlfall, T. L.; Lancaster, R. W.; Berg, R. W.; Strachan, C. J.; Pepper, M.; Gordon, K. C.; Rades, T. *J. Pharm. Sci.* **2006**, *95*, 2486.
(19) Ebbinghaus, S.; Kim, S. J.; Heyden, M.; Yu, X.; Heugen, U.; Gruebele, M.; Leitner, D. M.; Havenith, M. *Proc. Natl. Acad. Sci. U.S.A.* **2007**, *104*, 20749.
(20) Markelz, A. G.; Roitberg, A.; Heilweil, E. J. *Chem. Phys. Lett.* **2000**, *320*, 42.

(21) King, M. D.; Ouellette, W.; Korter, T. M. *J. Phys. Chem. A* **2011**, *115*, 9467.
(22) Allis, D. G.; Hakey, P. M.; Korter, T. M. *Chem. Phys. Lett.* **2008**, *463*, 353.
(23) Hakey, P. M.; Allis, D. G.; Hudson, M. R.; Ouellette, W.; Korter, T. M. *ChemPhysChem* **2009**, *10*, 2434.
(24) King, M. D.; Buchanan, W. D.; Korter, T. M. *J. Phys. Chem. A* **2010**, *114*, 9570.
(25) Grimme, S. *J. Comput. Chem.* **2004**, *25*, 1463.
(26) Grimme, S. *J. Comput. Chem.* **2006**, *27*, 1787.
(27) O'Brien, E. J. *Acta Crystallogr.* **1967**, *23*, 92.
(28) Rice, A.; Jin, Y.; Ma, X. F.; Zhang, X. C.; Bliss, D.; Larkin, J.; Alexander, M. *Appl. Phys. Lett.* **1994**, *64*, 1324.
(29) Wu, Q.; Litz, M.; Zhang, X. C. *Appl. Phys. Lett.* **1996**, *68*, 2924.
(30) King, M. D.; Buchanan, W. D.; Korter, T. M. *J. Pharm. Sci.* **2011**, *100*, 1116.
(31) Dovesi, R.; Orlando, R.; Civalleri, B.; Roetti, C.; Saunders, V. R.; Zicovich-Wilson, C. M. *Z. Kristallogr.* **2005**, *220*, 571.
(32) Dovesi, R.; Saunders, V. R.; Roetti, C.; Orlando, R.; Zicovich-Wilson, C. M.; Pascale, F.; Civalleri, B.; Doll, K.; Harrison, N. M.; Bush, I. J.; D'Arco, P.; Llunell, M. *Crystal09 User's Manual*; University of Torino: Torino, 2009.
(33) Perdew, J. P.; Burke, K.; Ernzerhof, M. *Phys. Rev. Lett.* **1996**, *77*, 3865.
(34) Krishnan, R.; Binkley, J. S.; Seeger, R.; Pople, J. A. *J. Chem. Phys.* **1980**, *72*, 650.
(35) Civalleri, B.; Zicovich-Wilson, C. M.; Valenzano, L.; Ugliengo, P. *CrystEngComm* **2008**, *10*, 1693.
(36) King, M. D.; Buchanan, W. D.; Korter, T. M. *Phys. Chem. Chem. Phys.* **2011**, *13*, 4250.
(37) Gilat, G. *J. Comput. Phys.* **1972**, *10*, 432.
(38) Monkhorst, H. J.; Pack, J. D. *Phys. Rev.* **1976**, *13*, 5188.
(39) Dovesi, R.; Pisani, C.; Roetti, C.; Saunders, V. R. *Phys. Rev. B: Condens. Matter* **1983**, *28*, 5781.
(40) Pascale, F.; Zicovich-Wilson, C. M.; Gejo, F. L.; Civalleri, B.; Orlando, R.; Dovesi, R. *J. Comput. Chem.* **2004**, *25*, 888.
(41) Dall'Olio, S.; Dovesi, R.; Resta, R. *Phys. Rev. B: Condens. Matter* **1997**, *56*, 10105.
(42) Ahmed, Z.; Chou, S. G.; Siegrist, K.; Plusquellic, D. F. *Faraday Discuss.* **2011**, *150*, 175.
(43) Bond, A. D.; Solanko, K. A.; van de Streek, J.; Neumann, M. A. *CrystEngComm* **2011**, *13*, 1768.